ELSEVIER

Fuel 79 (2000) 141–151

FUEL

www.elsevier.com/locate/fuel

Deposit formation on a single cylinder during combustion of herbaceous biomass

H. Kaufmann[a], Th. Nussbaumer[a,b,*], L. Baxter[c], N. Yang[c]

[a]*Swiss Federal Institute of Technology, ETH Zurich, CH-8092 Zurich, Switzerland*
[b]*Verenum Research, Langmauerstrasse 109, CH-8006 Zurich, Switzerland*
[c]*Sandia National Laboratories, Livermore, CA 94551-0969, USA*

Accepted 29 June 1999

Abstract

The combustion of herbaceous biomass can lead to deposit formation on the walls of the combustion chamber and on boiler tubes. These deposits are being caused by fly ash. The aim of the present investigation was to identify the mechanisms of deposit formation, to analyse the chemical and morphological properties of the deposit, and to propose measures for deposit reduction. Special attention was given to the deposit formation from flue gas having been cleaned from large particles. It is typically found in boilers from moving bed furnaces. Experiments were performed in the flue gas of a turbulent flow reactor by sampling the depositions on a cooled cylinder after having removed large particles on an obstacle. Furthermore, depositions from the boilers of two moving bed furnaces were collected. The investigations show that depositions similar to those in moving bed furnaces were achieved in the turbulent flow reactor when large particles were removed before sampling. The deposits from herbaceous biomass were identified as accumulations of fine particles in the nanometer range. The chemical properties of the deposits are those of KCl, the major compound in the deposit. Among the different formation mechanisms thermophoresis was revealed to be the crucial process for deposit formation under the investigated conditions.

Keywords: Biomass combustion; Deposit; Aerosol; Particle; Particle size; Thermophoresis

1. Introduction

Deposit formation on boiler tubes due to fly ash is an undesired side effect of the combustion process. Particularly herbaceous biomass causes intense deposit growth compared to other fuels such as wood or coal [1,2]. Deposit formation from herbage-grass or miscanthus was found to be approximately six times faster than from native wood. Since the adherence between the deposit and the boiler is rather weak, the injection of pressurised air can be applied to clean the deposit layers. However, due to the high gas temperature in the entrance zone of the boiler (>800°C), sintering or melting of the deposits can lead to glass-like layers, which can hardly be removed. The boiler performance is significantly reduced due to the reduced heat exchange. Therefore, deposit formation should be avoided by appropriate measures. The aim of the present investigation was to identify the relevant mechanisms of deposit formation under conditions as they are typically found in moving bed furnaces (grate and under stoker furnaces).

2. Theory

Four main release mechanisms are distinguished for the formation of fly ash from coal and biomass [3]: Evaporation from the fuel, disintegration from the fuel by chemical inorganic reaction, convective disintegration due to organic reactions or rapid devolatilization, and chemical transformation in the flue gas. Some inorganic compounds in the biomass are already evaporated into the flue gas in significant concentrations at temperatures as low as 500°C. Inorganic material can also devolatilize from entrained fuel particles or newly formed structures. Furthermore, local chemical reactions in the fuel lead to an almost constant stream of volatile inorganics under combustion conditions. An example for the fourth mechanism of fly ash production, the transformation by chemical reaction, is the reaction of KCl and SO_x leading to K_2SO_4 and HCl in the flue gas [4].

Deposit formation on obstacles has been investigated broadly, applying cylinders and spheres and involving

* Corresponding author. Tel.: +41-1-364-14-12; fax: +41-1-364-14-21.
E-mail address: verenum@access.ch (Th. Nussbaumer)

0016-2361/00/$ - see front matter
PII: S0016-2361(99)00137-4

Nomenclature

d	Diameter (m)
ER	Excess air ratio (dimensionless)
k	Heat conductivity (W/Km)
Kn	Knudsen number (dimensionless)
T	Temperature (°C)
v_0	Free flow speed (m/s)
Subscripts	
c	Cylinder
g	Gas
m	Mineral matter
p	Particle
Symbols	
η	Collection efficiency (dimensionless)
μ	Dynamic viscosity (Pa s)
ρ	Density (kg/m^3)
Λ	Mean-free path (m)

different particle collectives and flow conditions. Based on these experiments, the following mechanisms of particle deposition are distinguished [5]: Brownian diffusion, thermophoresis, electrophoresis, inertial impaction and gravity settling. The mechanisms are characterised by a dimensionless number, which is the ratio of the force causing particle deposition and the fluid friction of the continuous medium. To estimate the effect of the individual mechanisms, their collection efficiencies can be calculated. The collection efficiency is the ratio of the mass of collected deposit to the mass of fly ash available in the area covered by the protection cylinder in the direction of the gas flow.

Brownian diffusion is an important deposition mechanism for the condensation and solidification of fly ash vapour on cooled surfaces in combustion systems. Ranz [6] suggests Eq. (1) for the collection efficiency of the particle deposition on a single cylinder at $Re_c > 1$ (referring to the cylinder diameter) with the assumption, that the flow can be treated as a potential flow

$$\eta_{0,D} = (1 + R) - \frac{1}{(1 + R)} \tag{1}$$

R is the collection parameter $2x_0/d_c$, the ratio between the limiting distance from the cylinder surface at $\theta = \pi 2$ and the cylinder diameter for particles, which will be precipitated by diffusion. The theory allows a first rough approximation of $\eta_{0,D}$ by applying the basic knowledge going back to a suggestion from Langmuir [7]. He calculated R based on Eq. (2), where $\bar{x}$ is the particle displacement from the flow line due to the random movement during the time interval t

$$\bar{x} = \sqrt{\frac{4D_p t}{\pi}} \tag{2}$$

Using the Einstein–Stokes expression for the diffusion coefficient D_p and estimating the time t for $Re_c > 1$ (Langmuir considered $Re_c < 1$) the collection parameter R results from:

$$\frac{1}{2}R = \frac{x_0}{d_c} = \frac{1}{2}\left(\frac{3.52D_p}{v_0 d_c}\right)^{1/2} \tag{3}$$

To estimate the time t we assume that particles diffuse in a viscous flow to the cylinder in the angular section of $\theta = 30$ to 150° having the same tangential speed as the fluegas. Applying Eq. (3) in Eq. (1) the collection efficiency for diffusive particle transport to the cylinder surface can be calculated for the potential flow. The ratio $D_p/v_0 d_c$ in Eq. (3) is the dimensionless parameter N_{sd} of the diffusion effect as indicated in Eq. (4)

$$N_{sd} = \frac{CkT}{3\pi\mu d_p d_c v_0} \tag{4}$$

Electrophoresis is the motion of particles smaller than 0.1 μm influenced by electrostatic forces of the surrounding particles and surfaces. Particles in the fluegas of combustion systems are only weakly charged due to the diffusion of ions to the particle surface (ion diffusion) and possibly also due to electron exchange at fluid–solid interfaces followed by separation of the two phases (electrolytic mechanisms). Furthermore, the maximum possible electron charge per particle is rapidly decreasing to less than 10 for particles smaller than 0.1 μm as shown by Dennis [8]. The mechanistic aspect and physical limits suggest that electrostatic field forces in combustion systems are rather weak. To estimate the collection efficiency due to electrostatic forces, existing data referring to spherical collectors are used. The dimensionless parameter for electrophoresis has the form [9]:

$$N_{se} = \frac{CQ^2}{3\pi^2\mu\varepsilon_0 d_p d_c^2 v_0} \tag{5}$$

For the inertial impact, a comparison between experimental and theoretical collection efficiency can be done based on different empirical formulas. Here, the empirically obtained formulation from Langmuir and Blodgett [10] is used:

$$\eta_{0,I} = \frac{\mathrm{Stk}^2}{(\mathrm{Stk} + 0.25)^2} \tag{6}$$

The dimensionless Stokes' expression for the relaxation time, Stk, also stands for the dimensionless inertial parameter as defined in Eq. (7). It represents the ratio of the force which is necessary to stop a spherical particle in the distance of a characteristic size of the obstacle (if the obstacle is a cylinder the characteristic size is, e.g. $d_c/2$) to the fluid friction at a relative speed of v_0 [15]

$$\mathrm{Stk} = N_{si} = \frac{C\rho_p d_p^2 v_0}{18\mu d_c} \tag{7}$$

Gravity settling can be neglected. The corresponding dimensionless similarity parameter N_{sg} is the ratio of gravity

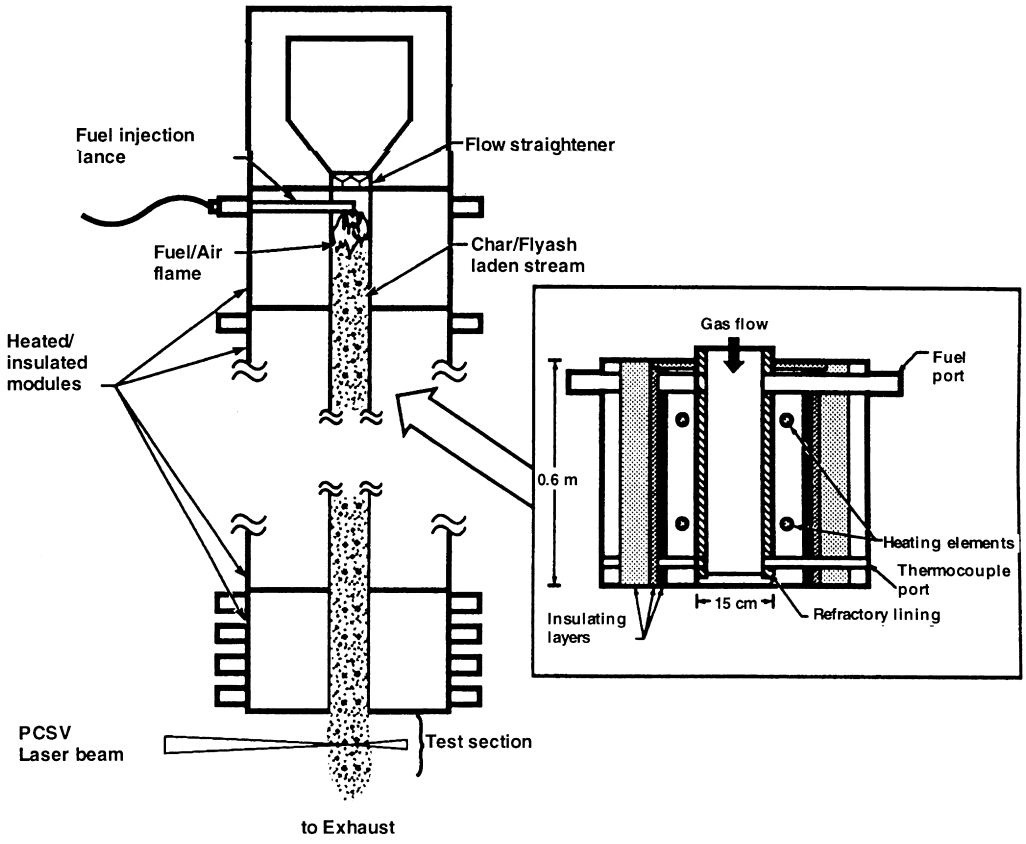

Fig. 1. Laboratory turbulent flow reactor (MFC) at Sandia National Laboratories.

to fluid friction on a spherical particle (Eq. (8)). For the size range assumed for fly ash particles N_{sg} is at least one order of magnitude smaller than the analogue parameter for inertial impaction

$$N_{sg} = \frac{C\rho_p d_p^2 g}{18\mu v_0} \tag{8}$$

Thermophoresis is caused by the temperature gradient in the fluegas near cooled surfaces [5]. Particles in this transition zone are attracted by the wall due to the unequal momentum transfer by the non-uniform energy distribution among the surrounding gas molecules. For slip flow ($Kn \leq 1$) the thermophoretical attraction will be much stronger than near the continuum range ($Kn \gg 1$). The dimensionless thermophoretical parameter N_{st} is defined as the ratio of the thermophoretic force to the fluid friction for v_0

$$N_{st} = \left(\frac{T_g - T_c}{T_g}\right)\left(\frac{\mu}{C\rho d_p v_0}\right)\left(\frac{k_g}{2k_g + k_c}\right) \tag{9}$$

The collection efficiency is calculated based on the diffusion collection efficiency using a 'thermal suction' factor f_s suggested by Rosner [5]. This factor allows a linear correction of the diffusive mass transfer, represented by $Nu_{m,0}$, for the simultaneous effect of thermophoresis (Nu_m) :

$$Nu_m = Nu_{m,0} f_s \tag{10}$$

with

$$f_s = \frac{Pe_s}{1 - e^{-Pe_s}} \tag{11}$$

Pe_s is the Peclet number calculated from the thermophoretic drift speed $(\alpha_T D)_p \nabla T/T$ in the boundary layer around the obstacle and the particle Diffusion coefficient D_p. The thermal diffusivity, $(a_T D)_p$, of the drift speed is calculated after Talbot et al. [11]:

$$(\alpha_T D)_p = \frac{2C_s v\left(\frac{k_g}{k_p} + C_t Kn\right)[1 + Kn(A + Be^{-CR/\lambda})]}{(1 + 3C_m Kn)(1 + 2\frac{k_g}{k_p} + 2C_t Kn)} \tag{12}$$

3. Experimental investigation

The aims of the experiments are:

- identifying of the controlling fly ash release mechanisms by comparing the physical and chemical nature of the deposits with the one of the fuel itself;
- identifying the controlling deposit formation mechanisms based on the morphological characteristics size and particle shape and verifying these mechanisms with the collection efficiency.

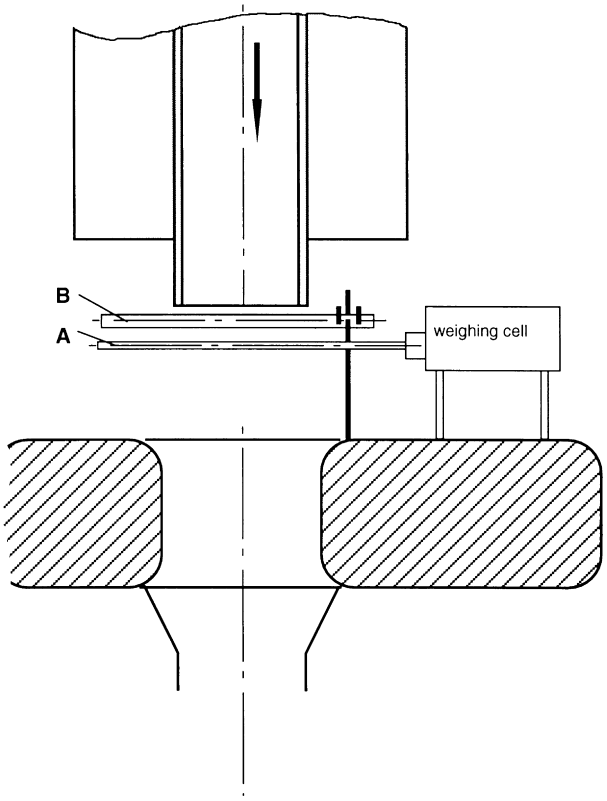

Fig. 2. Arrangement of sampling cylinder A and protection cylinder B in the outlet of the MFC.

The influence of the combustion conditions was taken into account by designing the experiments for two different levels of the excess air ratio (ER = 1.4 and 2.2), which is the basic parameter for the optimisation of the combustion process [12].

To obtain results of general validity for different combustion systems, deposit collection by a cylinder was used as a well proven sampling technique, which is broadly used as representative model for steam pipes in boilers.

To reach the first goal, the experiments were designed to show the context between the inorganic fuel elements and the deposit composition. Consequently, deposit samples from the cylinder were analysed for their elemental composition and chemical structure. The second goal was approached using the structure and growth of the deposit on the single cylinder to give the basic data for the collection efficiency and the morphological characteristics.

Experiments were planned for laboratory scale, choosing the turbulent flow reactor of Sandia National Laboratories (multi fuel combustor, MFC, Fig. 1). The vertical combustor is designed for the undisturbed observation of deposit formation in a duct. Sampling and measurement in the flue gas can be made without restriction by limiting reactor walls [3]. The investigated fuels were herbage-grass, miscanthus and pine with a particle size smaller than 2 mm.

To investigate the reliability of the deposit sampling technique, deposits from smokepipes of a moving grate furnace and an underfeed stoker furnace were analysed for their chemical composition and morphological characteristics. These results were compared to those of the single cylinder deposits to show the degree of equivalency. Detailed information about the experiments with the moving bed furnaces and the sampling procedure are presented in Ref. [4].

3.1. Experimental equipment

The turbulent flow reactor, described in detail in earlier reports [3,13], is 4.2 m long and 0.12 m wide. The wall temperature of the cylindrical reactor can be heated up to 1000°C and the fuel powder is fed pneumatically into the top section.

The deposit formation was analysed on an air-cooled single cylinder, which was arranged in the fluegas from herbage-grass, miscanthus and wood at the end of the combustor (Fig. 2). This arrangement allowed in situ measurement of deposit growth, surface temperature and characteristic infrared emission spectra and the sampling of representative deposits for chemical and morphological analysis. The following measurement techniques were used: chemical disintegration analysis for elemental composition of solids, X-ray diffraction for crystalline compounds (XRD) in solids, continuous registration of the cylinder's weight for deposit growth by means of an electromagnetic mass compensation weighing cell, and dual-wavelength infrared measurement for surface temperature of the deposit. Cross section cuts of sampling cylinder B after the experiments were investigated by scanning electron microscopy (SEM) and the SEM photographs evaluated for particle shape and size.

Combustion in a grate furnace leads to a different distribution of the ash effluent from the fuel than in the MFC. In the grate furnace, fly ash devolatilizes from the burning fuel, which moves slowly along the grate. At the end of the grate large ash particles leave the system as powdery or sintered grate ash. In the MFC fly ash and grate-ash are not separated. Since only fly ash is responsible for the observed deposit formation in grate furnaces, an appropriate sampling in the MFC is needed to collect only the fly ash fraction comparable to a grate furnace.

In the turbulent flow reactor "grate" and "fly" ash can be separated due to the different particle inertia. This working hypothesis is based on the assumption that the heavy non-volatile inorganic compounds of the biomass usually found in the grate ash would form conglomerates with diameters much bigger than the diameter of typical fly ash particles [3]. Knowing that the densities of fly ash and grate ash substances do not differ tremendously, the separation of the two ash fractions simply would depend on the particle size.

A simple, but very efficient method to separate particles in a suspension according to their mass inertia is an abrupt

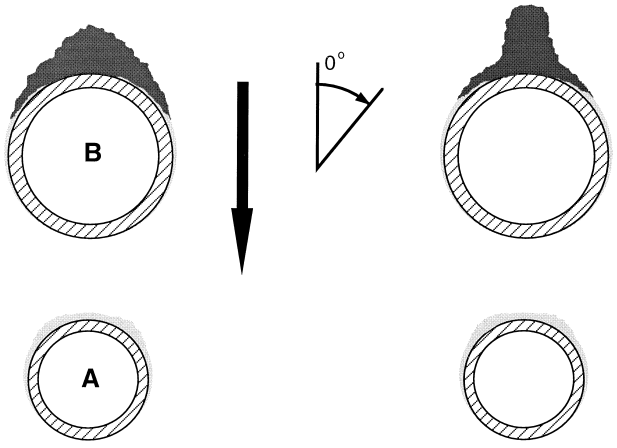

Fig. 3. Cross section view of the fly ash deposits on cylinder A and B from miscanthus (left) and herbage-grass (right).

change of the flow direction. For the presented investigation, two cylinders lying in series perpendicular to the flow direction of the fluegas accomplish this effect. The sheltered cylinder A is used for sampling and measurement purposes (Fig. 2).

4. Results

The following results, revealed from single cylinder experiments, present the characteristics of the fly ash deposits. In comparison to the experiments with herbage-grass and miscanthus, the deposit formation due to wood combustion is too small to allow reliable analysis with the chosen arrangement. Nevertheless, results from herbage-grass and miscanthus combustion are also relevant for wood as the smokepipe results from the full scale experiments with the 450 kW_{th} grate furnace and the 100 kW_{th} underfeed stoker furnace implies [4,14].

The results are presented using the following arrangement for general terms and parameters. The two chosen levels of the excess air ratio are distinguished by 'low ER' and 'high ER'. 'Low ER' (1.3–1.5) corresponds to incomplete combustion, 'high ER' (2–2.3) is equal to complete or good combustion. Polar coordinates are commonly used to describe cylinder deposit formations. The stagnation point on the front side is defined to be the angle $\theta = 0°$. The expression 'fly ash' is strictly used to describe the inorganic, volatile emission from biomass combustion, which solidifies in the fluegas after the furnace.

4.1. Morphological characteristics of the deposits

Macroview Macroscopic cross section views of the deposits on cylinders A and B, as shown in Fig. 3, indicate the effect of fuel type on deposit shape. Large particles impacted on the front side of cylinder B form a steep pile in case of herbage-grass and a rather evenly distributed pile in case of miscanthus. Particles settling on cylinder B beyond an angle of $\pm 60°$ from the stagnation point of the stream and those on cylinder A have formed a smooth and sticky white layer, which is the desired fly ash deposit as shown by microscopic investigations. The excess air ratio did not have a visible influence on the appearance of the deposit.

Microview for herbage-grass combustion, SEM-analysis of the cross section cuts through a cylinder in position B revealed the particle sizes in the loose layer on the front side and in the lateral sticky layer. Whereas, the loose deposit contains particles with a diameter well above 100 μm (Fig. 5), the sticky layer contains particles with a typical size of 100–300 nm (Fig. 4).

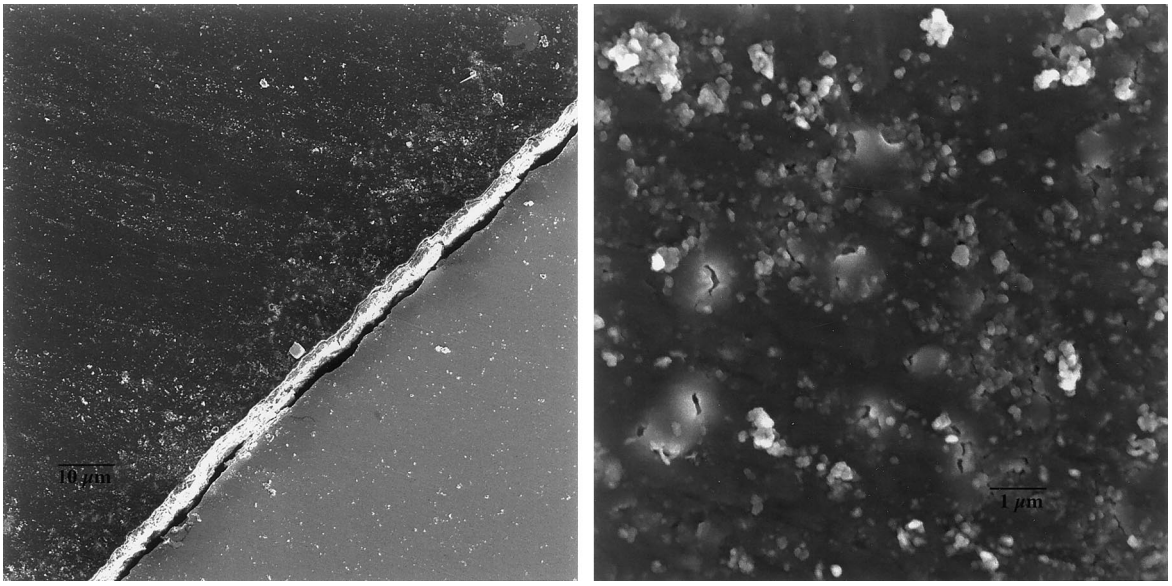

Fig. 4. Cross section view of the sticky deposit on cylinder B at ER = 2.2 (left) and with enlarged details of the enlighted square (right).

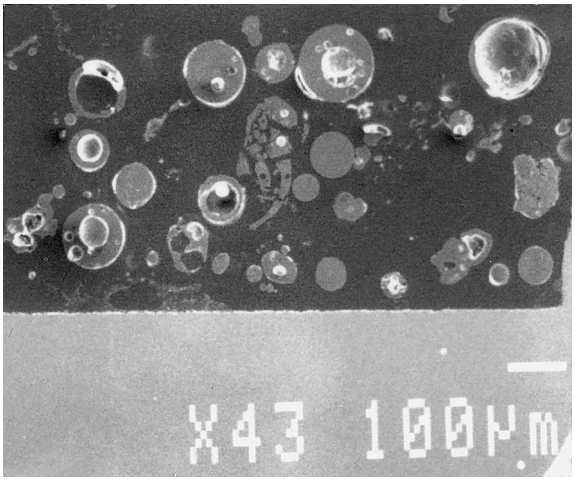

Fig. 5. Front side deposit on cylinder B after combustion of miscanthus at ER = 2.2.

The particles in the sticky deposit have an almost point-symmetric, cubic shape which was also observed for fly ash particles collected earlier in the fluegas of a 50 kW_{th} underfeed stoker furnace, and for the particles in the boiler deposit of the 100 kW_{th} underfeed stoker furnace mentioned above (Fig. 6). The investigation of the boiler deposits has also indicated, that the excess air ratio affects the particle size but not their shape. Decreasing excess air ratio leads to increasing particle size (200–500 nm) compared to the size mentioned above.

The particle distribution over cylinder A shows a good separation between heavy and light particles through inertial impaction on the front side of the cylinder. SEM-pictures from a cross section cut through the deposit from herbage-grass (at low ER) show, that the heavy particles on the front side are 100–1000 times bigger than the light particles in the sticky deposit. Since the sticky deposit is formed in a parallel stream analogously to smokepipe deposits and since the morphological deposit characteristics are similar in both cases, it must be the very fine fly ash particles that cause the sticky deposit.

Resuming the observations, the deposit investigation by means of two cylinders arranged in series (Figs. 2 and 3) delivers a sticky deposit beyond $\pm 60°$ which has the same typical shape and size as particles in boiler deposits and fly ash from furnaces having a fuel bed. Consequently, following analysis is concentrated on the sticky deposit.

4.2. Elemental composition of deposit and fuel

K, Si and Cl are the main fractions of the deposit, independent of the fuel (Table 2), and KCl and K_2SO_4 were the identified crystalline compounds. Differences are due to differences of the corresponding elemental fuel composition and the combustion conditions (Table 1). The detected Si fraction is most probably part of the amorphous solids containing mainly potassium and oxygen. In comparison with herbage-grass, deposits from miscanthus contain more silica than potassium. This is consistent with the fact that miscanthus has a much higher degree of lignification

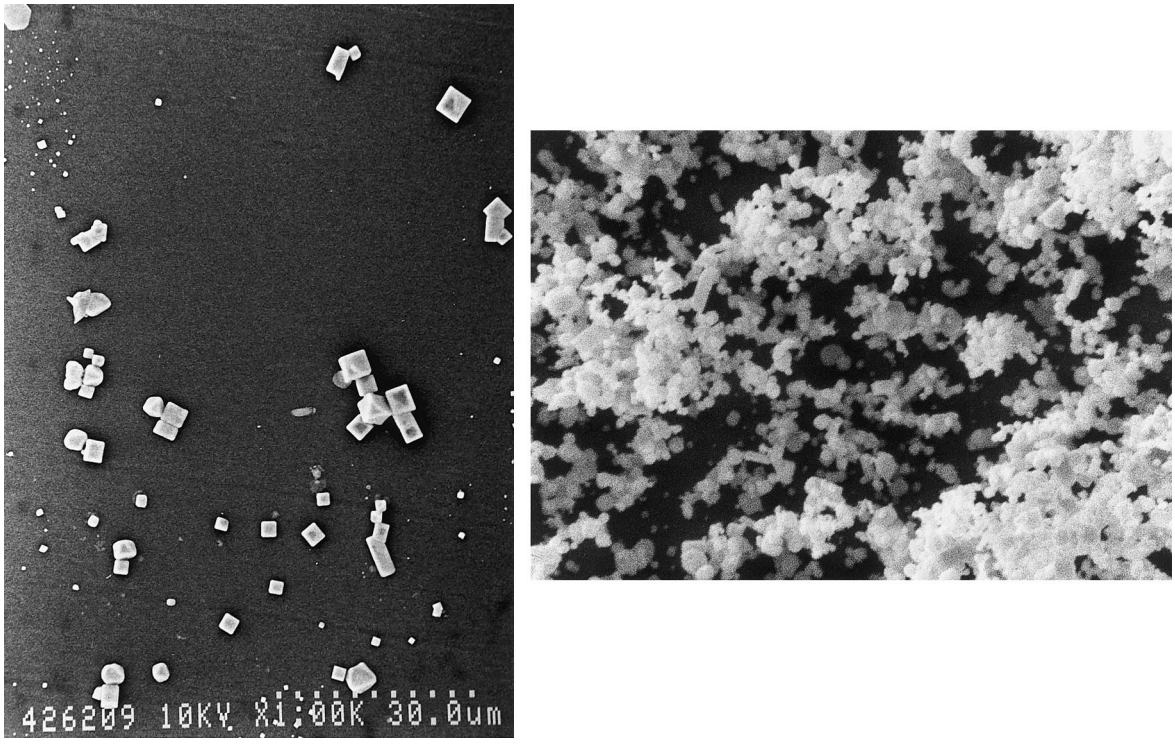

Fig. 6. Fly ash (left) and smokepipe deposit particles (right) from the underfeed stoker furnace at ER = 2.2.

Table 1
Fuel composition in (wt.%)

Fuel	Herbage-grass (wt.%)	Miscanthus (wt.%)	Wood (wt.%)
Humidity	11.15	10.61	9.67
Ash	7.34	3.66	0.41
Ash elements		m	
K	1.92	0.383	0.032
S	0.107	0.035	0.002
Cl	0.352	0.063	0.002
Si	1.08	0.855	0.042
Ca	0.818	0.174	0.061
Na	0.027	0.522	0.001
P	0.208	0.047	0.002
Mg	0.193	0.04	0.031
Ti	0.009	0.001	< 0.00004
Fe	0.069	0.037	0.004
Al	0.11	0.013	0.005
C	46.53	49.16	52.14
N	1.28	0.31	0.09
H	5.51	5.57	5.83
Sum of elements	58.2	57.2	58.2

and thus a lower content of potassium and chloride than herbage-grass.

At low excess air ratio (ER = 1.2), Si was detected at significantly higher mass fraction than at high excess air ratio (ER = 2.2) (Table 2). This effect is also observed for S, Ca and Na, while K and Cl have shown the opposite behaviour: at low excess air ratio their mass fractions were lower than at high ER. Resuming the observation, the deposit mass was similar in both cases but contained a higher mineral fraction at low ER than at high ER. Taking into account that the unknown rest of the deposits is most probably oxygen, this effect confirms the assumption that the devolatilization rate of mineral elements from biomass increases with increasing combustion temperature caused by decreasing excess air ratio.

About 0.2–0.5 wt.% of the total mineral content in the biomass contributed to the deposit formation on cylinder A. Smokepipe deposits from the grate furnace reached about 0.7–1.1 wt.%. The difference is due to the incomplete sampling of sedimented particles in the case of the cylinder, since the applied procedure did not include the particles, which settled on the front side of the cylinder.

The comparison with results from the 450 kW_{th} grate furnace reveals a very close chemical relationship between the front side deposit and grate ash on the one side and between sticky deposit and smokepipe deposit on the other (Fig. 7, Table 2). However, Si appeared in cylinder deposits at significantly higher levels than in boiler deposits. This is possibly related to the less effective separation of refractory material in our simple experiments compared to commercial operation.

The mass fraction of carbon did not exceed 0.05% in any of the deposits on the cylinder and in the smokepipes. This confirms the assumption that solids containing major amounts of carbon are not existing in the fluegas if the combustion is operated at optimum conditions.

At fluegas temperatures between 600 and 700°C, the deposit surface on the cooled cylinder reaches temperatures between 400 and 450°C. As required for the experiments, these temperature conditions correspond to the conditions in hot water boilers.

4.3. Collection efficiency and deposit growth

The collection efficiency of cylinder A did neither show a strong dependence on the type of fuel nor on the excess air ratio. Data from on-line weighing suggest linear growth of the deposit mass with exposure time.

Table 2
Composition of the sticky deposit on a single cylinder in the turbulent flow reactor compared to the composition of deposits in the boiler of a 450 kW_{th} grate furnace in (wt.%)

Fuel	Herbage-grass			Miscanthus		
Dep.	MFC, sticky deposit		Boiler	MFC, sticky deposit		Boiler
ER Dim.	1.2–1.5 (wt.%)	2–2.3 (wt.%)	2–2.3 (wt.%)	1.2–1.5 (wt.%)	2–2.3 (wt.%)	2–2.3 (wt.%)
K	27.72	30.1	43.2	10.3	12.1	21.09
S	6.76	1.94	3.29	11.5	1.45	2.38
Cl	12.4	13	23.9	2	8.37	11.08
Si	18.25	10	4.17	21.7	20.5	13.09
Ca	9.58	7.51	1.96	4.57	5	5.47
Na	0.82	1.16	0.816	11.5	1.13	0.831
P	4.62	2.59	1.52	1.39	1.49	1.49
Mg	2.82	2.15	0.663	1.13	1.16	1.43
Ti	0.086	0.07	0.012	0.04	0.04	0.108
Fe	1.23	0.7	0.595	1.12	1.26	4.86
Al	0.84	1.32	0.153	0.8	0.79	0.69
C	0.13	0.4	0.027	0.48	0.75	0.055
Sum:	85.3	70.9	80.3	66.5	54	62.6

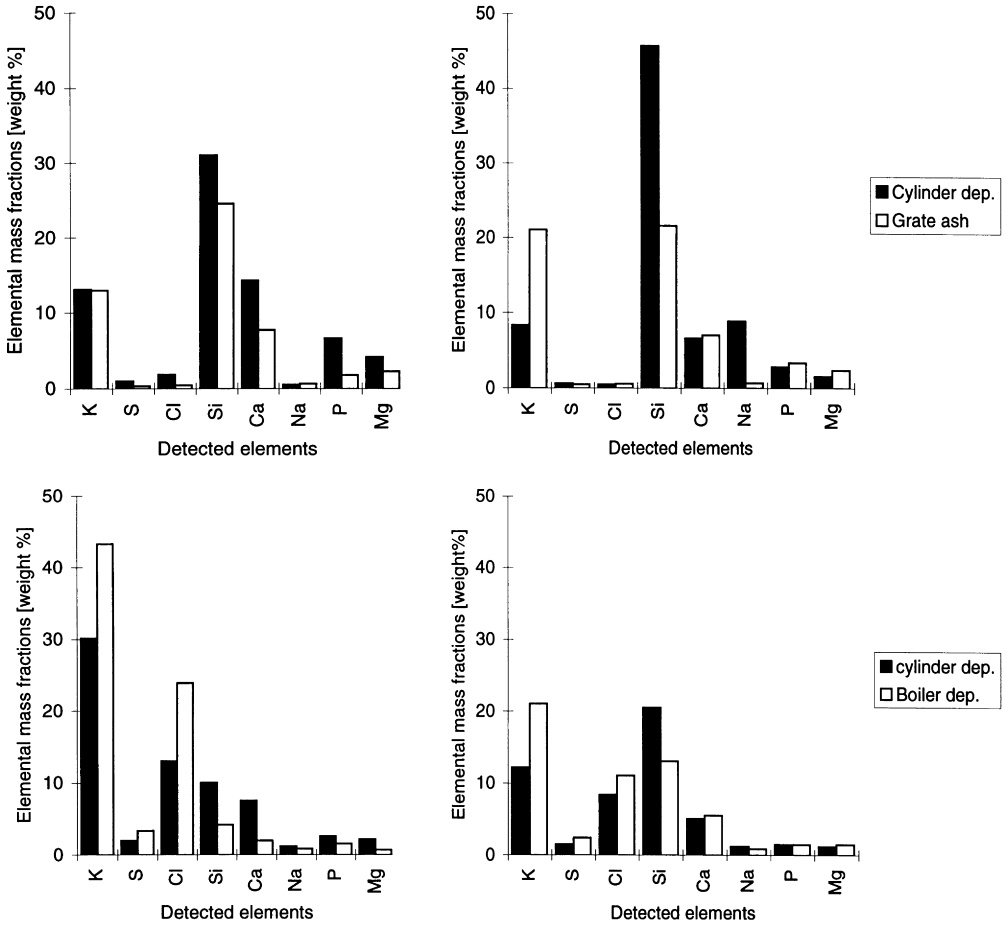

Fig. 7. Comparison between important elements in deposits from the MFC and the 450 kW_{th} grate furnace for herbage-grass (left) and miscanthus (right) at ER > 2. Above: front side and grate ash deposits. Below: sticky and smokepipe deposits.

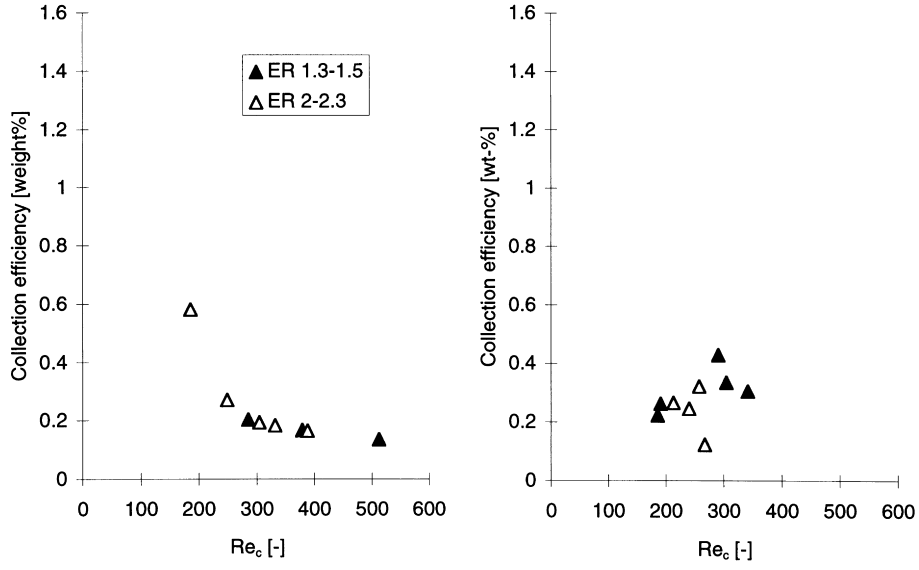

Fig. 8. Collection efficiency for herbage-grass (left) and miscanthus (right).

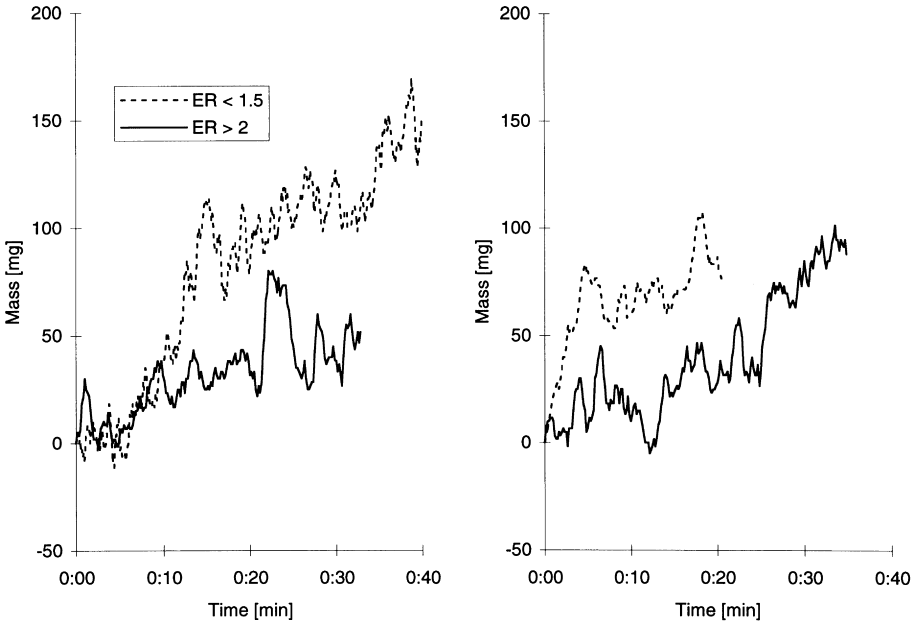

Fig. 9. Deposit growth for herbage-grass (left) and miscanthus (right).

Collection efficiency. The collection efficiency of cylinder A was between 0.1 and 0.4% for herbage-grass and between 0.1 and 0.6% for miscanthus. For herbage-grass the collection efficiency clearly decreased with increasing Reynolds number for the cylinder diameter or analogously with increasing free flow speed of the fluegas around the cylinder (Fig. 8). Data from miscanthus did not show a clear trend with the Reynolds number. Assuming similar behaviour in both cases the results for herbage-grass deposits suggests two possible reasons for the observed dependency:

Due to friction settled particles are rather re-entrained into the fluegas flow at high *Re* than at low *Re*.

With increasing *Re* the fluegas speed increases, but not the settling speed of the particles. Since such small particles have almost the same speed as the flue gas (the relative speed to the fluegas flow is independent from the gas speed [5]), their residence time near the obstacle surface decreases with increasing *Re* leading to fewer particles being settled per unit volume of the fluegas flow.

Table 3
Parameters for the calculation of the theoretical deposit growth (typical composition of biomass fluegas (N_2,H_2O,O_2,CO_2))

ρ_p (kg/m^3)	1500	d_c (m)	0.017
ρ_g (kg/m^3)	0.394	T_g (°C)	600
d_p (m)	5×10^{-8}	T_c (°C)[a]	500
k_m (W/Km)	1	T_c (°C)[b]	400
v_0 (m/s)	2	Re_c (dimensionless)	300
k_g (W/K m)[a]	0.058	Λ (m)[c]	0.245×10^{-6}
μ (Pa s)	1.24×10^{-5}	C (dimensionless)[c]	0.059

[a] Cooled by natural convection.
[b] Cooled with pressurized air at 25°C.
[c] Air.

For the calculation of the collection efficiency, the sticky deposit must be separated from the front deposit [15].

Deposit growth. Based on the continuous weight data for the total deposit mass, the sticky deposit is assumed to grow linearly with time for both herbs (Fig. 9). Typical growth rates were 1.6 mg/min for herbage-grass and 2.4 mg/min for miscanthus (ER = 2.2). The linear behaviour of the total deposit growth could be investigated during a maximum stationary time interval of 2 h and after an initial start-up time of 20–30 min. Results from the grate furnace show the same trends at slightly higher levels.

The values for the growth of the sticky deposit result from the mass after the experiments and the measured collection time, assuming linear relation between growth and time as observed for the total deposit mass on cylinder A.

4.4. Formation mechanisms

The formation mechanisms were examined for their theoretical contribution to the deposit growth in order to estimate their relevance in relation to the measured total deposit growth. Using the equations for the collection efficiencies presented earlier, the deposit growth was estimated based on particle and fluegas properties.

All calculations have been done for an undisturbed laminar potential flow around a single cylinder. The deposit parameters (Table 3) necessary for the calculation of the theoretical deposition efficiencies were based on the data from our experiments (d_p, d_f, v_0, T_g, T_c) and the data from literature (ρ_p, η_g, $c_{p,g}$, C, Λ). Based on this data set, the theoretical values for the collection efficiency of the single mechanisms are as given below.

Inertial impaction calculated after Langmuir (Eq. (7)):

$$\eta_{0,I} = 8.65 \times 10^{-13}$$

Gravity settling can be neglected since the influence of gravitation on the particle motion is approximately 25 times smaller than the inertial effect as the comparison of the respective deposit parameters (Eqs. (8) and (7)) for our case ($v_0 = 2$ m/s, $d_c = 0.017$ m) revealed.

Interestingly, precipitation by *diffusion* (Eq. (1)) reaches a collection efficiency of at least 10^{-4}

$$\eta_{0,D} = 2.24 \times 10^{-4}$$

Despite the small diffusion collection efficiency, newer suggestions for the simulation of the inertial influence on deposit formation [5] indicate that diffusion may have a more important contribution to the deposit formation in turbulent than in laminar flows. Since the deposit collection happened in a turbulent flow, the calculated collection efficiency would have to be corrected for eddy diffusion. Yet, compared to other formation mechanisms, the corrected efficiency would still be very small, as other studies indicate [5].

An estimation for the collection efficiency due to *electrophoresis* clearly indicates that this effect is negligible for particles in the submicron range. Referring to Dennis [8], we were supposing a maximum charge of 8×10^{-19} C on the particles

$$N_{se} = 1.6 \times 10^{-12}$$

The small value of N_{se} calculated for an uncharged, spherical collector ([9], see theory), suggests an inferior significance of electrophoresis. The efficiency is far below 10^{-5} for the particles found in our experiments.

In case of cooling by forced convection deposit growth due to *thermophoresis* was seen to be about 1000 times more intensive than by diffusion alone. This factor was calculated after Rosner (Eqs. (10) and (11)) for the two cooling cases: air cooling inside the cylinder by natural (open cylinder) and forced convection ($V^* = 45$ l/min, $T_{air} = 25$°C). Based on the measured metal surface temperature, the ratio of the initial collection efficiencies of thermophoresis and of diffusion then becomes:

$$\eta_{0,T}/\eta_{0,D} = 280$$

(Natural convection cooling, $\Delta T/T = 0.2$)

$$\eta_{0,T}/\eta_{0,D} = 700$$

(Forced convection cooling $\Delta T/T = 0.5$)

where ΔT is the temperature difference between cylinder surface and fluegas and T the fluegas temperature.

Obviously, cooling by forced convection should attract more than twice as much particles than cooling by natural convection. With a mean particle size of approximately 200 nm and an estimated mean free path length of 250 nm, thermophoresis definitely acts under slip flow conditions in combustion systems.

Both, the theoretical and the experimental collection efficiency have the dimension 10^{-2}. The theoretical approach enhances the assumption that thermophoresis and most probably eddy diffusion are the main deposition mechanisms whereas inertial impact, gravity settling and electrophoresis can be neglected for practical operation. Deposit growth by thermophoresis would be expected to become less significant as deposits grow and surface temperature increases. Curiously, no such trend was observed. Other recent investigations observe the same trend and indicate that thermophoresis is not as well understood as we thought [15].

5. Conclusions

Fly ash solidifies in flue gas and collects on the cylinder surface due to the low temperatures (600–750°C). With respect to the particle shape and size found in the deposits, their chemical composition and the lack of an important electric field, the relevant deposition mechanism with comparable theoretical collection rate for the single cylinder is thermophoresis.

Gravitational and inertial effects can be excluded for the observed deposit formation since the particle size is far too small for a significant deposit formation. The specific, solid particle state leads to negligible transport effect of diffusion and thermodiffusion. Since theoretically possible electric charges on the walls of the combustion systems and on the particle surface are very small, no important transport effect can be contributed by electrophoresis.

The close relationship between deposit and fly ash material confirms the assumption that the settling particles are identical to fly ash. Investigations of boiler deposits from the combustion of herbage-grass in a grate furnace show similar characteristics as the single cylinder deposits and confirm the negligible influence of gravitation and inertial effects on the particle sedimentation.

Since only diffusive transport mechanisms are relevant for the precipitation of the deposit from particles in the nanometer range, they can only be precipitated from the fluegas flow if their residence time is high. Another promising way would be to agglomerate the particles, which however demands high pressure. If applied in front of the boiler, such innovative methods would reduce the deposit formation and the whole fly ash emission, but also demand measures to improve the economic value of the combustion system to reimburse the additional investment.

More promising in terms of investment for technical equipment would be the prevention based on pre-combustion measures, such as selective application and harvesting of biomass or artificial reduction of the mineral content of the fuel [4]. Morphology and chemical analysis confirm the

assumption, that the entrained ash in the MFC is separated into fractions equivalent to ‘grate ash-like’ and ‘fly ash-like’ by means of the here applied serial cylinder arrangement.

Acknowledgements

The present investigation was funded by the Swiss Federal Office of Energy. The experiments with the grate furnace were carried out in cooperation with SCHMID AG and TIBA-MUELLER AG (Switzerland).

References

[1] Biollaz S, Nussbaumer T. Einsatz von Rostfeuerungen für Holz und Halmgüter. In: 4. Holzenergie-Symposium, ETH Zurich 18 October 1996. p. 9–42.
[2] Christensen K. The formation of submicron particles from the combustion of straw, PhD thesis, Technical University of Denmark, Lyngby, 1995.
[3] Baxter LL. Ash deposition during biomass and coal combustion: a mechanistic approach. Biomass and Bioenergy 1993;4(2):85–102.
[4] Kaufmann H. Chlorine compounds in emissions and residues from the combustion of herbaceous biomass. PhD thesis 12429, Swiss Federal Institute of Technology, Zurich, 1997.
[5] Rosner DE. Transport processes in chemically reacting flow systems, London: Butterworths, 1986.
[6] Ranz W. Technical Report No. 3, Contract AT-(30-3)-28, University of Illinois, 1951.
[7] Langmuir I. Filtration of aerosols and the development of filter materials, OSRD-Report No. 865, 1942.
[8] Dennis R. Handbook on aerosols TID-26608, Technical Information Centre, Office of Public Affairs, US Energy Research and Development Administration, 1976.
[9] Kraemer HF. Collection of aerosol particles in presence of electrostatic fields. Industrial and Engineering Chemistry 1955;47(12).
[10] Langmuir I, Blodgett B. Mathematical investigation of water droplet trajectories, Report No. RL-225, General and Electric Research Laboratory, 1945.
[11] Talbot L, Cheng R, Schefer R, Willis D. Thermophoresis of particles in a heated boundary layer. Journal of Fluid Mechanics 1980;101(4):737–58.
[12] Nussbaumer Th. Wood combustion. Advances in thermochemical biomass conversion, Glasgow: Blackie, 1994 p. 575–89.
[13] Baxter LL, Jenkins BM, Miles TR, et al. Alkalis in alternative biofuels. FACT, vol. 18, Combustion modeling, scaling and air toxins, ASME, 1994.
[14] Kaufmann H, Nussbaumer Th. Characteristics and formation of fly ash particles in biomass furnaces. In: Biomass for energy and industry. 10th European Conference and Technology Exhibition. 8–11 June, Würzburg, 1998. p. 1326–9.
[15] Sinquefield SA, Baxter LL, Frederick WJ. An experimental study of the mechanisms of fine particle deposition in kraft recovery boilers. In: Tappi proceedings 1998. International Chemical Recovery Conference. Tampa, vol. 2, 1–4 June, 1998. p. 443–67.